T and NK cell immunity after hematopoietic stem cell transplantation

Lugthart, G.

Chapter 6

Expansion of cytotoxic CD56^{bright} NK cells during T cell deficiency after allogeneic hematopoietic stem cell transplantation

Published in:
Journal of Allergy and Clinical Immunology
2017; 140: 1466-1469

Gertjan Lugthart
Marieke Goedhart
Merle M. van Leeuwen
Janine E. Melsen
Cornelia M. Jol-van der Zijde
Carly Vervat
Monique M. van Ostaijen-ten Dam
Anja M. Jansen-Hoogendijk
Maarten J.D. van Tol
Arjan C. Lankester *and*
Marco W. Schilham

Abstract

We describe a compensatory expansion of activated cytotoxic CD56^{bright} NK cells during T-cell deficiency after hematopoietic stem cell transplantation. This mimics the situation in severe inborn T-cell deficiencies and unmasks the functional and phenotypic versatility of NK cells.

To the editor:

Cytokine-producing, non-cytotoxic CD56^{bright}CD16$^{+/-}$ (CD56^{bright}) NK cells constitute a minor population of NK cells in blood of healthy individuals.[87;95;97] Both early after hematopoietic stem cell transplantation (HSCT) and in patients with severe inborn T-cell deficiencies, NK cells are skewed towards the CD56^{bright} NK cell phenotype.[126;127;216;234] These clinical situations are marked by the absence of T-cells. The role of NK cells in immunity may normally be overshadowed by the presence of T cells. Therefore, transient T-cell deficiency after HSCT provides an opportunity to unveil compensatory adaptations in the CD56^{bright} NK cell compartment.

We evaluated the reconstitution of T and NK cells in ninety-three pediatric acute leukemia patients who received an HSCT from a matched-unrelated donor (MUD) or HLA-identical related donor (IRD). See Supplemental Data for methods and cohort description. Delayed T-cell reconstitution was defined as <100 T-cells/µl at four weeks after HSCT and occurred in 33 patients (35%). In patients with a delayed T-cell reconstitution, CD56^{bright} NK cells expanded to high numbers, reaching median 320 cells/µl (range 5-1255) at four weeks after HSCT. In contrast,

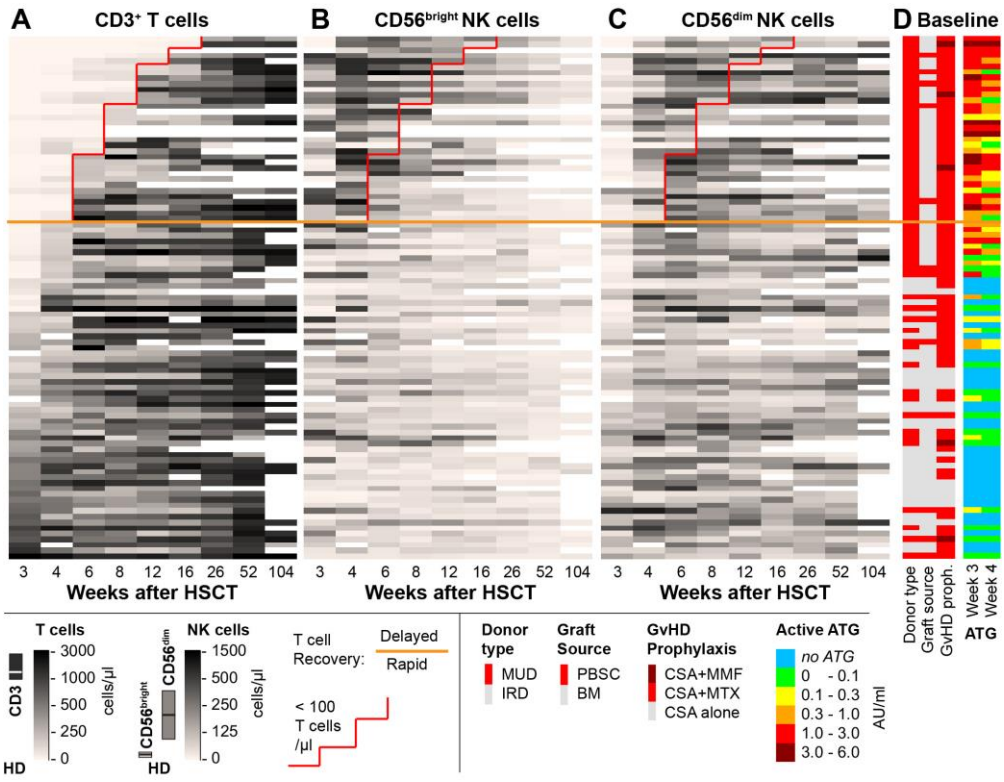

Figure 6.1. Expansion of CD56^{bright} NK cells in patients with delayed T-cell reconstitution.

(A-C) Reconstitution of T-cells (A), CD56^{bright} (B) and CD56^{dim} NK cells (C) in 93 HSCT recipients. Each row represents a patient. Patients were sorted by T-cell reconstitution. HD values are shown in legend.

(D) Side bars displaying donor type, graft source, graft versus host (GvHD) prophylaxis and active (T-cell binding) ATG concentration. Abbreviations: PBSC: peripheral blood stem cells, BM: bone marrow, CSA: cyclosporin A, MTX: methotrexate, MMF: mycophenolate mofetil, AU: arbitrary units.

this strong expansion of CD56^{bright} NK cells was only observed in a minority of patients with a rapid T-cell reconstitution (Figure 6.1B and Figure 6.S1A). CD56^{bright} NK cell numbers remained high until T-cell reconstitution occurred, as demonstrated by inverse log-linear correlation between T-cell numbers and CD56^{bright} NK cell numbers at 4, 8, 12 and 16 weeks after HSCT (Figure 6.1A-B and Figure 6.S1B). The skewing towards CD56^{bright} NK cells after HSCT is often used to support the hypothesis that CD56^{bright} NK cells are the precursors of CD56^{dim} NK cells. However, recovery of CD56^{dim} NK cells after HSCT was independent of T-cell reconstitution (Figure 6.1C and Figure 6.S1A,C), arguing against a sequential reconstitution of CD56^{bright} and CD56^{dim} NK cells.

We compared patients with >300 CD56^{bright} NK cells/μl in the first 3-6 weeks after HSCT (n=38) to those without CD56^{bright} NK cell expansion (<300 CD56^{bright} NK cells/μl, n=55) to study the correlation with various other HSCT parameters. In multivariate analysis, CD56^{bright} NK cell expansion was only correlated with the use of anti-thymocyte globulin (ATG) serotherapy (overlapping with MUD donors, $p<0.001$) and the absence of T-cells at four weeks after transplantation ($p=0.002$, Table 6.S1). Because ATG serotherapy leads to delayed T-cell reconstitution[30;33], we conclude that delayed T-cell reconstitution represents the main determinant of the expansion of CD56^{bright} NK cells.

Next, we measured the longitudinal expression of 34 chemokine-receptors, adhesion-molecules and NK cell markers on CD56^{bright} NK cells from HSCT recipients (n=20) and healthy donors (HD, n=16). *t*-SNE analysis visualizing these phenotypic data revealed that CD56^{bright} NK cells at 3-4 weeks after HSCT differed from CD56^{bright} NK cells in steady state conditions (Figure 6.2A-B). Post-transplant CD56^{bright} NK cells had a significantly increased expression of inflammatory chemokine-receptors (CCR2, CCR5 and CX3CR1) and the skin-specific cutaneous lymphocyte antigen (CLA, Figure 6.2B and Figure 6.S2). CLA and CX3CR1 were transiently expressed, while other receptors remained high for weeks (CCR5) or months (CCR2). This suggests specific regulation of individual chemokine-receptor expression rather than a general activation of NK cells. Interestingly, post-transplant CD56^{bright} NK cells had a reduced expression of the chemokine-receptors CCR7 and CXCR3, indicating reduced homing to lymphoid organs (Figure 6.2B). Together, these data emphasize that post-transplant CD56^{bright} NK cells have adopted the phenotype of effector cells.

Post-transplant CD56^{bright} NK cells lacked the early differentiation markers CD127 and CD27. A proportion of these cells expressed KIRs and CD57, late differentiation markers normally only expressed by CD56^{dim} NK cells. This suggests that post-transplant CD56^{bright} NK cells are more differentiated than HD CD56^{bright} NK cells, although the expression of these markers can also be affected by *in vitro* activation.[97;127]

Conventional CD56^{bright} NK cells are abundant cytokine producers but do not express granzyme B at rest, requiring pre-activation to obtain cytolytic potential.[87;95] The IFN-γ and TNF-α production and perforin expression of NK cells early after HSCT was comparable to healthy donors (Figure 6.2C and E3).[126;127] However, post-transplant CD56^{bright} NK cells expressed granzyme B at rest (94 vs 15% (HD), *p=0.002*, Figure 6.2D). Accordingly, they were cytotoxic without pre-activation. Their cytotoxicity was comparable to NK cells from three or more months after HSCT and healthy donors, both containing predominantly CD56^{dim} NK cells (Figure 6.2E).

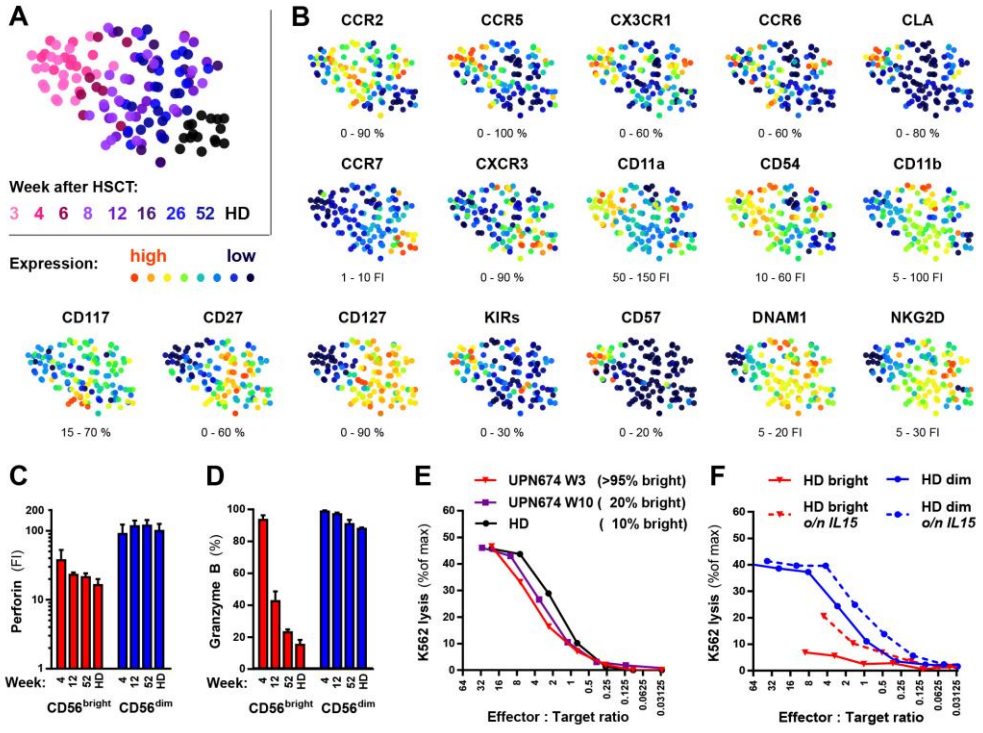

Figure 6.2. Phenotype and function of CD56^{bright} NK cells after HSCT

(A-B) *t*-SNE analysis of the expression of 34 cell-surface markers on CD56^{bright} NK cells in 134 samples from 20 HSCT recipients and 16 HD. Distance between dots indicates the difference in phenotype. Plots are colored by time after HSCT (A) and marker-expression (B). Range: percentage or fluorescence-intensity (FI). For gating strategy and non-depicted markers: see Supplemental Data.

(C-D) Intracellular expression of granzyme B and perforin in NK cells at 4, 12 and 52 weeks after HSCT (n=3) and HD (n=3). Bars: mean +/- SEM.

(E-F) Cytotoxicity of: (E) unmanipulated PBMC 3 and 10 weeks after HSCT and HD (Week 3: >95% CD56^{bright}). (F) Resting and overnight IL15-activated FACS-purified HD NK cells. Representative graphs of three (E) and two (F) experiments.

In contrast, purified HD CD56^{bright} NK cells were only cytotoxic after overnight activation with IL15 (Figure 6.2F). Together, the functional profile of post-transplant CD56^{bright} NK cells corresponds with that of conventional, cytokine secreting CD56^{bright} NK cells that have acquired cytolytic potential, most likely as result of *in vivo* activation.

Various studies have highlighted the inferior outcome of patients with a delayed T-cell reconstitution after ATG serotherapy.[30;33] In subgroup analysis, transplant-related mortality, leukemia-relapse and overall-survival were comparable between patients with rapid T-cell reconstitution (n=60) and patients with a delayed T-cell reconstitution but with CD56^{bright} NK cell expansion (n=26, Table 6.S2). Only patients lacking both rapid T-cell reconstitution and CD56^{bright} NK cells expansion (n=7) had a high mortality. This suggests that NK cells may be able to bridge the T-cell deficient period after HSCT.

The expansion of activated CD56^{bright} NK cells with increased effector characteristics in the setting of T-cell deficiency could be elicited by infectious or non-infectious inflammatory triggers. In view of the role of NK cells in antiviral immunity, it is possible that the expansion of CD56^{bright} NK cells is driven by viral infections which frequently occur in the T-cell deficient period after HSCT.

Our data are in line with the reported observations in patients with severe inborn or acquired T-cell deficiencies. In patients with RAG and ARTEMIS deficiencies, an increased proportion of NK cells had the CD56^{bright} phenotype, and these cells degranulated strongly upon coculture with K562.[235] In HIV patients, an inverse correlation between CD4^{+} T-cell numbers and CD56^{bright} NK cells was observed. These cells also had a reduced expression of CCR7 and an increased expression of granzyme B.[236]

Together with the changes in the NK cell compartment in other T-cell deficient situations, our data demonstrate that CD56^{bright} NK cells form a versatile cell population which can expand and acquire additional effector functions in the absence of T-cells. The reactive changes in the NK cell compartment may represent a compensatory response of NK cells to inflammatory or infectious triggers when T-cells are not present to exert their function. The setting of T-cell deficiency provides a unique opportunity to further study the biology of human NK cells and their role in human disease.

Acknowledgements

The authors thank Prof. dr. F. Koning, dept. of immunohematology and blood transfusion, LUMC, Leiden, the Netherlands for critical reading of the manuscript

Funding and Disclosures

Research was financially supported with a grant from the Dutch Cancer Society (#UL 2011-5133). GL was supported by a Leiden University Medical Center MD/PhD fellowship.

Supplemental data

Supplemental Methods

Patients, blood samples and ethics statement

Between 1-1-2005 and 31-12-2014, 99 pediatric acute lymphoblastic leukemia (ALL) or acute myeloid leukemia (AML) patients received a bone marrow (BM) or peripheral blood stem cell (PBSC) graft from an identical related (IRD) or matched unrelated donor (MUD) after myeloablative conditioning in the Leiden University Medical Center. Only patients who received anti-thymocyte globulin (ATG, Thymoglobulin, Genzyme, Cambridge, MA, USA) or no serotherapy were evaluated (n=94). Patients were only included after their first transplantation. One patient who died within one week after HSCT was excluded, resulting in a cohort of 93 patients. Patients received a graft from a matched-unrelated donor (MUD, n=60) or HLA-identical related donor (IRD, n=33). MUD transplantation was always combined with ATG serotherapy. 15 patients received a peripheral blood stem cell graft graft, the remaining 78 patients received a BM graft. The median age was 9.2 years (range 0.8-17.8).

All transplantations were performed according to national protocols and in line with the recommendations of the European group for Blood and Marrow Transplantation. Peripheral blood samples taken at 3, 4, 6, 8, 12, 16, 26, 52 and 104 weeks after HSCT were evaluated. Follow up ended earlier when leukemia relapsed (n=20) or the patient died (n=10). Blood samples were freshly analyzed. In addition, blood samples were cryopreserved and used for phenotypic and functional analyses with approval of the institutional review board (protocol P01.028). Informed consent was obtained from all patients and/or their parents or legal guardians.

Monitoring of immune reconstitution

To monitor immune reconstitution, peripheral blood white blood cell counts including full leukocyte differentiation were performed weekly. Freshly isolated peripheral blood mononuclear cells (PBMC) were analyzed by flow cytometry to determine the size of different lymphocyte populations and subsets. PBMC were separated from EDTA blood using ficoll-isopaque density gradient centrifugation (LUMC Pharmacy, Leiden, NL) and stained with antibodies as listed in Table 6.S3. Four-color flow cytometry was performed on a BD FACS Calibur II flow cytometer (Becton Dickinson Biosciences (BD), Franklin Lakes, NJ, US) and data were analyzed using BD Cellquest software. Lymphocytes were defined as $CD45^+$ CD33/CD235a/$CD14^-$ cells within the forward / sideward scatter lymphocyte gate. T cells and NK cells were defined as $CD3^+$ cells and $CD3^-CD56^+$ cells in the lymphocyte population, respectively. In a separate tube, $CD56^{bright}CD16^{+/-}$ and $CD56^{dim}CD16^+$ NK cells were gated within the $CD3^-CD14^-$ lymphocyte gate (Figure 6.S4 A-B).

Multicolor flowcytometry

The expression of 42 cell surface markers (17 chemokine receptors, 10 adhesion molecules and 15 NK cell markers) was measured on $CD56^{bright}$ and $CD56^{dim}$ NK cells in a subgroup of 20 HSCT recipients and 16 healthy donors. For this, patients were selected that did not receive prednisolone. Cryopreserved PBMC were thawed and subjected to a three step staining procedure after 1h recovery at 37°C / 5% CO_2 in AIM-V medium (Life Technologies) with 10% fetal calf serum (FCS, GE Hyclone, Logan, UT, US). All antibodies used are listed in Table 6.S3. PBMC were first incubated with unconjugated antibodies, washed twice and stained with fluorochrome-labeled secondary antibodies. For the third step, PMNC were stained with directly labeled antibodies in the presence of normal mouse serum (5% (v/v), Seralab, London, UK). Prior to analysis, DAPI (25 ng/ml, Sigma-Aldrich) was added.

Data were acquired on a LSR II flow cytometer (Becton Dickinson (BD), Franklin Lakes, NJ, US) using FACS Diva Software (v6.1, BD). Data were acquired on different days, but with the same instrument settings. For each experiment, spectral overlap was compensated based on single stained cells. All samples from an individual patient were measured in a single experiment. The cell surface marker panel was validated for the use on cryopreserved cells by the comparison between fresh and cryopreserved PBMC from four healthy donors and two HSCT recipients at one month after HSCT. We excluded $CD56^{dim}CD16^{-}$ NK cells from further phenotypic characterization as they constituted a separate population in cryopreserved but not in fresh PBMC.[237] Also, CD49b was excluded from further analysis because the expression of this marker was significantly reduced on cryopreserved cells (data not shown). The other markers could be measured reliably on cryopreserved NK cells.

The gating strategy is depicted in Figure 6.S4C. $CD56^{bright}CD16^{+/-}$ and $CD56^{dim}CD16^{+}$ NK cells were defined as living, non-doublet $CD3^{-}CD7^{+}$ lymphocytes expressing CD56 and/or CD16. Flow cytometric data were analyzed using Kaluza software (v1.3, Beckman Coulter, Brea, CA, US). For each NK cell population, the expression of the cell surface markers was calculated as follows: for cell surface markers with a bimodal expression, the percentage of positive cells minus isotype control was calculated; for markers with a continuous expression, the ratio of geomean fluorescence intensity of marker and isotype control (FI) was calculated.

t-SNE analysis of cell surface receptor expression data

We used *t*-distributed stochastic neighbor embedding (t-SNE) analysis to visualize the flowcytometry data.[238;239] The population expression profile of 34 cell surface markers on $CD56^{bright}$ NK cells from 134 blood samples of 20 patients and 16 healthy donors were combined in this t-SNE analysis. The following markers were included in the analysis: chemokine receptors CCR2, CCR5, CCR6, CCR7, CXCR1, CXCR2, CXCR3, CXCR4, CXCR6 and CX3CR1; adhesion molecules cutaneous lymphocyte antigen (CLA), Integrin β7 (ITGB7), CD11a, CD11b, CD31, CD44, CD49d, CD54 and CD162; NK cell receptors CD27, CD57, CD69, CD94, CD117, CD127, NKp30, NKp44, NKp46, NKp80, NKG2A, NKG2C, NKG2D, DNAM1 and pan-KIR mix. CD56 and CD16 were not included in the t-SNE analysis as these markers were used for the population definition. The cell surface markers CCR1, CCR3, CCR4, CCR8, CCR9, CCR10,

CXCR5 and CD103 were not included in the t-SNE analysis because these receptors were neither expressed on CD56^{bright} nor on CD56^{dim} NK cells. For missing data, the average expression of the cell surface marker on the concerning NK cell subset at that time point was used.
Population expression data (percentage or FI) for each marker were normalized on a scale from 0-100, with each value expressed as a percentage of the range between the highest and the lowest value. Two-dimensional Barnes-Hut *t*-SNE analysis was performed.[240;241] Plots show all individual samples and are based on the *t*-SNE field parameters V1 and V2. Because of the random effect in t-SNE analysis, 20 runs of t-SNE were performed, all resulting in comparable plots. Afterwards, dots were colored to highlight different time-points (Figure 6.1A). The relative expression of individual cell surface markers was plotted in separate dot plots (Figure 6.1B). To reduce the visual impact of outliers to the color-coding display, the very low (<p2.3) and very high (>p97.7) values for each cell surface marker were replaced by the p2.3 and p97.7 value after the *t*-SNE analysis but before the construction of plots of individual cell surface marker expression.

In vitro assessment of cytotoxicity and cytokine production

To assess the cytotoxic potential of post-transplant CD56^{bright} NK cells, PBMC from 3 patients with >95% CD56bright NK cells at 1 month after HSCT were used in a chromium release assay and compared with PBMC from 3 months after HSCT (with CD56^{dim} and CD56^{bright} NK cells) and with healthy donor PBMC. After thawing, cells were rested overnight in AIM-V medium with 10% FCS in 96-well round bottom plates (Greiner Bio-One, Kremsmünster, Austria).and their cytotoxicity against K562 cells was evaluated in a 4h chromium release assay as previously described.[242] The cytotoxicity of unselected NK cells from PBMC was compared to the cytotoxicity of purified healthy donor CD56^{bright} and CD56^{dim} NK cells. For this, CD56^{bright} and CD56^{dim} NK cells were purified by fluorescence activated cell sorting (FACS) from freshly isolated healthy donor PBMC as described previously,[243] and rested overnight in the absence or presence of IL15 (10 ng/ml, Cellgenix, Freiburg, Germany).
Cytokine production of post-transplant CD56^{bright} NK cells was evaluated in PBMC from three patients at 1, 3 and 12 months post HSCT and 2 healthy donors. 2-4x10^5 PBMC were cultured in AIM-V medium with 10% FCS for 16-18h. Cells were either unstimulated (medium) or stimulated with recombinant human IL12 (10 ng/ml, Peprotech, Rocky Hill, NJ, US), IL15 (10 ng/ml), IL18 (20 ng/ml, MBL International, Woborn, MA, US) or combinations of these monokines. BD golgistop (1:1500, BD) was added during the last 4h of culture. Cells were harvested, stained for cell surface markers, fixed and permeabilized and stained for intracellular interferon-γ and tumor necrosis factor-α (IFN-γ & TNF-α, Table 6.S3) in a paraformaldehyde/ saponin based intracellular staining protocol as previously described.[244]

Measurement of active ATG concentrations

Patients receiving a stem cell graft from a MUD received ATG at a cumulative dose of 10 mg/kg body weight in 3-4 doses from day -5 to -1 pre-HSCT. Active ATG levels were routinely measured using quantitative flow cytometry assays as previously described.[33] Active ATG was

defined as the fraction of the product capable of binding to the HUT-78 T cell line. In short, HUT cells were incubated with fourfold dilutions of patient serum, washed and incubated with Alexa Fluor 647 (A647) labeled goat anti-rabbit IgG (Life Technologies, Carlsbad, CA, USA). Subsequently, cells were washed and the FI for A647 was measured by flow cytometry on a BD FACS Calibur II flow cytometer. To construct a reference curve, HUT cells were incubated in 25% pooled human serum supplemented with known amounts of ATG straight from the vial of the supplier. Active ATG was measured in arbitrary units (AU). Five mg/ml ATG was arbitrarily set at containing an active ATG concentration of 5000 AU/ml.[33]

Data analysis and statistics

Data were analyzed and figures were constructed in R (version 3.3.2, 64 bit; R Foundation, Vienna, Austria) and GraphPad Prism (Version 7.02, GraphPad Software, San Diego, CA, US). Data were pre-processed using the R package dplyr [245] Barnes-Hut *t*-SNE analysis was performed using the R package Rtsne.[240] Heatmaps and dot plots were built using the R packages Heatmap3, ggplot2 and Rcolorbrewer.[246-248] Linear regression analysis on log-transformed data was used to evaluate the correlation between T- and NK cell numbers. Univariate associations between HSCT characteristics and the hyperexpansion of $CD56^{bright}$ NK cells after HSCT (>300 cells/ µl) were evaluated using logistic regression analysis. The Firth penalized likelihood bias-reduction method was applied for categorical variables with complete data separation using the R package logistf.[249] Parameters with *p-values <0.10* in univariate analysis were included in a multivariate logistic regression analysis using backward stepwise elimination. For subgroup analysis, chi-square test was used to compare the distribution of categorical parameters between all 4 groups and (combinations of) subgroups. Unpaired t tests on log-transformed data were used to compare cell numbers and cell surface marker expression on $CD56^{bright}$ NK cells between patient samples and/or healthy donors. *P-values <0.01* were considered statistically significant. The Bonferroni-Holm method was used to correct for multiple comparisons.[250]

	CD56^{bright} NK cells >300 cells/µl (n=38)		CD56^{bright} NK cells <300 cells/µl (n=55)		*p value*	
Baseline	***N***	**%**	***N***	**%**	*Univariate*[1]	*Multivariate*[2]
Donor type[3] ***MUD*** *(vs. IRD)*	*37*	97.4%	*23*	41.8%	*<0.001*	*NA*[3]
Graft Source ***PBSC*** *(vs. BM)*	*9*	23.7%	*6*	10.9%	*0.100*	*NS*
GvHD Prophylaxis[4] *CSA+MTX*	*35*	92.1%	*36*	65.5%	*0.001*	*NS*[4]
CSA alone	*0*	0.0%	*17*	30.9%		
CSA+MMF	*3*	7.9%	*2*	3.6%		
Serotherapy[3] ***ATG*** *(vs. none)*	*37*	97.4%	*23*	41.8%	*<0.001*	<0.001
<100 T cells/µl at week 4	*26*	68.4%	*7*	12.7%	*<0.001*	0.002
	Median	***Range***	**Median**	***Range***		
ATG conc. at week 3 *(AU/ml)*	1.12	*0 - 5.9*	0.32	*0 - 4.9*	*0.016*	*NS*
ATG conc. at week 4 *(AU/ml)*	0.39	*0 - 3.7*	0.06	*0 - 1.7*	*0.032*	*NS*
Age *(years)*	7.7	*0.8 - 17.7*	10.7	*0.8 - 17.8*	*0.042*	*NS*
Outcome	***N***	**%**	***N***	**%**	*Univariate*	*Multivariate*[5]
CMV viremia *(2x>10^3 copies/ml)*	*6*	15.8%	*8*	14.5%	*0.870*	
EBV viremia *(2x>10^3 copies/ml)*	*13*	34.2%	*6*	10.9%	*0.006*	*0.15*
hAdV viremia *(2x>10^3 copies/ml)*	*4*	10.5%	*4*	7.3%	*0.580*	
Acute GvHD *(grade II-IV)*	*6*	15.8%	*16*	29.1%	*0.140*	*0.64*
Chronic GvHD *(extended)*	*3*	7.9%	*6*	10.9%	*0.440*	
Leukemia relapse	*7*	18.4%	*14*	25.5%	*0.430*	
Transplant related mortality	*2*	5.3%	*5*	9.1%	*0.490*	
One year survival	*33*	86.8%	*44*	80.0%	*0.390*	
Overall survival	*26*	73.7%	*37*	67.3%	*0.510*	

Table 6.S1. Comparison of HSCT recipients with and without CD56^{bright} NK cell hyperexpansion

Baseline characteristics and outcome parameters of HSCT recipients with and without hyperexpansion of CD56^{bright} NK cells (>300 cells/µl) within six weeks after HSCT. *p* values: [1]Univariate logistic regression analysis and [2]multivariate logistic regression analysis using backward stepwise elimination. [3]All MUD and none of the IRD graft recipients received ATG serotherapy. [4]The Firth penalized likelihood bias-reduction method was applied for categorical variables with complete data separation (CSA alone). [5]For outcome parameters, NK cell hyperexpansion was corrected for delayed T cell reconstitution in multivariate logistic regression analysis.

Abbreviations: MUD: matched unrelated donor, IRD: HLA identical related donor, PBSC: peripheral blood stem cells, BM: bone marrow, CSA: cyclosporin A, MTX: methotrexate, MMF: mycophenolate mofetil, ATG: anti-thymocyte globulin, AU: arbitrary units, CMV: cytomegalovirus, EBV: Epstein-Barr virus, hAdV: human adenovirus, NS: not significant.

Table 6.S2. Subgroup analysis of outcome parameters

Subgroup analysis of outcome parameters between HSCT recipients with a rapid (group I, II) and delayed (group III, IV) T cell reconstitution, with (group I, III) and without (group II, IV) CD56^{bright} NK cell hyperexpansion. Rapid and delayed T cell reconstitution were defined as > or < 100 T cells / µl at 4 weeks after HSCT. Hyperexpansion of CD56^{bright} NK cells was defined as >300 CD56^{bright} NK cells / µl within six weeks after HSCT. Statistics: [1]chi square test comparing 4 groups and [2]chi square test comparing 2 groups. Abbreviations: CMV: cytomegalovirus, EBV: Epstein-Barr virus, hAdV: human adenovirus, GvHD: graft versus host disease.

	Group I		Group II		Group III		Group IV				
	T cells > 100/µl at week 4				**T cells < 100/µl at week 4**						
	NK > 300/µl		**NK < 300/µl**		**NK > 300/µl**		**NK < 300/µl**				
	n = 12		n = 48		n = 26		n = 7				
Outcome	**N**	**%**	**N**	**%**	**N**	**%**	**N**	**%**	***I vs. II vs. III vs. IV*[1]**	***III vs. (I+II)*[2]** *T-NK+ vs. T+*	***IV vs. (I+II)*[2]** T-NK- vs. T+
CMV viremia *(2x>10^3 copies/ml)*	*2*	16.7%	*7*	14.6%	*4*	15.4%	*1*	14.3%	*p value*[1] *1.0*	*p value*[2] *0.96*	*p value*[2] *0.96*
EBV viremia *(2x>10^3 copies/ml)*	*3*	25.0%	*4*	8.3%	*10*	38.5%	*2*	28.6%	***0.019***	***0.004***	*0.22*
hAdV viremia *(2x>10^3 copies/ml)*	*1*	8.3%	*4*	8.3%	*3*	11.5%	*0*	0.0%	*0.83*	*0.64*	*0.43*
Acute GvHD *(grade II-IV)*	*3*	25.0%	*15*	31.3%	*3*	11.5%	*1*	14.3%	*0.26*	*0.067*	*0.38*
Chronic GvHD *(extended)*	*1*	8.3%	*6*	12.5%	*2*	7.7%	*0*	0.0%	*0.72*	*0.58*	*0.34*
Leukemia relapse	*1*	8.3%	*12*	25.0%	*6*	23.1%	*2*	28.6%	*0.73*	*0.89*	*0.77*
Transplant related mortality	*1*	8.3%	*3*	6.3%	*1*	3.8%	*2*	28.6%	*0.17*	*0.61*	*0.055*
One year survival	*11*	91.7%	*41*	85.4%	*22*	85.6%	*3*	42.9%	***0.032***	*0.80*	***0.004***
Overall survival	*9*	75.0%	*34*	70.8%	*19*	73.1%	*3*	42.9%	*0.43*	*0.89*	*0.12*

Table 6.S3 (next pages). Antibodies used for flow cytometry

Staining was performed in a 96-well round-bottom plate with 0.5-1.5x106 cells in 25 µl per well for 30 min at 4°C in FACS buffer (Phosphate Buffered Saline (PBS, Braun, Melsungen, Germany) with bovine serum albumin (5 mg/ml, Sigma-Aldrich, St. Louis, MO, US) and sodium-azide (1 mg/ml, LUMC Pharmacy)) 1All four PE-conjugated α-KIR antibodies were combined in a pan-KIR staining. CD: Cluster of differentiation. n/a: not applicable. m: mouse, r: rat. Fluorochromes: AF: Alexa Fluor, APC: Allophycocyanin, BV: Brilliant Violet, ECD: Energy Coupled Dye (=Phycoerythrin-Texas Red conjugate), FITC: Fluorescein isothiocyanate, PE: Phycoerythrin, PE-Cy5.5: Phycoerythrin-Cyanine5.5 conjugate, PE-Cy7: Phycoerythrin-Cyanine7 conjugate, PERCP-Cy5.5: Peridinin Chlorophyll-Cyanine5.5 conjugate, RD-1: Red Dye 1. Companies: Ancell: Ancell Corporation (Bayport, MN, USA), BC: Beckman Coulter (Brea, CA, USA), BD: Becton Dickinson Biosciences (San Jose, CA, USA), Biolegend: Biolegend (San Diego, CA, USA), DAKO: Dako Denmark, (Glostrup, Denmark), eBioscience: eBioscience (San Diego, CA, USA), Invitrogen: Invitrogen (Thermo Fisher Scientific, Waltham, MA, USA), Miltenyi: Miltenyi Biotec, (Bergisch Gladbach, Germany), R&D: R&D Systems (Minneapolis, MN, USA), Sanquin: Sanquin Reagents (Amsterdam, Netherlands), Southern: Southern Biotech (Birmingham, AL, USA).

Table 6.S3. Antibodies used for flow cytometry

CD designation	Alternative name	Fluorochrome	Type	Clone	Company	Catalog#	Staining step
CD014	CD14	PE	m-IgG1	MφP9	BD	342408	Fresh Tube 1, Direct
CD033	SIGLEC3	PE	m-IgG1	P67.6	BD	345799	Fresh Tube 1, Direct
CD045	PTPRC	FITC	m-IgG1	2D1	BD	342408	Fresh Tube 1, Direct
CD056	NCAM1	APC	m-IgG1	N901	BC	IM2474	Fresh Tube 1, Direct
CD235a	GPA	PE	m-IgG1	11E4B-7-6	BC	A07792	Fresh Tube 1, Direct
CD003	CD3	PERCP-Cy5.5	m-IgG1	SK7	BD	340949	Fresh Tube 1+2, Direct
CD014	CD14	APC	m-IgG1	MφP9	BD	345787	Fresh Tube 2, Direct
CD016	FcγRIII	FITC	m-IgG1	3G8	BC	IM0814U	Fresh Tube 2, Direct
CD056	NCAM1	RD-1	m-IgG1	N901	BC	6603067	Fresh Tube 2, Direct
CD162	PSGL1	Unconjugated	m-IgG1	5D8-8-12	BC	IM2091	Primary
CD181	CXCR1	Unconjugated	m-IgG2a	42705	R&D	MAB330	Primary
CD182	CXCR2	Unconjugated	m-IgG2a	483112	R&D	MAB331	Primary
CD183	CXCR3	Unconjugated	m-IgG1	1C6	BD	557183	Primary
CD184	CXCR4	Unconjugated	m-IgG2b	44716	R&D	MAB172	Primary
CD185	CXCR5	Unconjugated	m-IgG2b	51505	R&D	MAB190	Primary
CD186	CXCR6	Unconjugated	m-IgG2b	56811	R&D	MAB699	Primary
CD191	CCR1	Unconjugated	m-IgG2b	53504	R&D	MAB145	Primary
CD192	CCR2	Unconjugated	m-IgG2b	48607	R&D	MAB150	Primary
CD194	CCR4	Unconjugated	m-IgG1	1D1	BD	551121	Primary
CD195	CCR5	Unconjugated	m-IgG2b	45531	R&D	MAB182	Primary
CD196	CCR6	Unconjugated	m-IgG2b	53103	R&D	MAB195	Primary
CD199	CCR9	Unconjugated	m-IgG2a	112509	R&D	MAB179	Primary
n/a	Isotype M-IgG1	Unconjugated	m-IgG1	11711	R&D	MAB002	Primary
n/a	Isotype M-IgG2a	Unconjugated	m-IgG2a	DAK-GO5	DAKO	X0943	Primary
n/a	Isotype m-IgG2b	Unconjugated	m-IgG2b	DAK-GO9	DAKO	X0944	Primary
n/a	Goat α m-IgG2b	AF488	polyclonal		Invitrogen	A21141	Secondary
n/a	Goat α m-IgG2b	AF647	polyclonal		Invitrogen	A21242	Secondary
n/a	Goat α m-IgG2b	PE	polyclonal		Southern	1092-09	Secondary
Secundary	Goat α M-IgG1	AF647	polyclonal		Invitrogen	A21240	Secondary
Secundary	Goat α M-IgG2a	AF647	polyclonal		Invitrogen	A21241	Secondary
CD003	CD3	BV510	m-IgG1	UCHT1	Biolegend	300448	Direct, basis
CD007	GP40	Alexa700	m-IgG1	M-T701	BD	561603	Direct, basis
CD016	FcγRIII	BV711	m-IgG1	3G8	BD	563127	Direct, basis
CD056	NCAM1	ECD	m-IgG1	N901	BC	A82943	Direct, basis
CD011a	LFA1	FITC	m-IgG1	HI111	BD	555383	Direct
CD011b	MAC1	FITC	m-IgM	1, B2	Sanquin	M1668	Direct
CD027	TNFRSF7	APC	m-IgG1	L128	BD	337169	Direct
CD031	PECAM1	PE	m-IgG1	WM59	BD	555446	Direct
CD044	HCAM	FITC	m-IgG1	J.173	BC	IM1219	Direct
CD049b	ITGA2	PE	m-IgG2a	12F1	BD	555669	Direct
CD049d	ITGA4	PE	m-IgG2b	L25	BD	340296	Direct

Table 6.S3. Antibodies used for flow cytometry (continued)

CD designation	Alternative name	Fluorochrome	Type	Clone	Company	Catalog#	Staining step
CD054	ICAM1	PE	m-IgG1	HA58	BD	555511	Direct
CD057	B3GAT1	FITC	m-IgM	HNK1	BD	347393	Direct
CD069	EA-1	FITC	m-IgG1	L78	BD	347823	Direct
CD094	KLRD1	PE	m-IgG1	HP-3D9	BD	555889	Direct
CD103	ITGAE	FITC	m-IgG1	BER-ACT8	DAKO	F7138	Direct
CD117	c-kit	PE	m-IgG1	104D2	BD	332785	Direct
CD127	IL7Rα	FITC	m-IgG1	eBioRDR5	eBioscience	11-1278	Direct
CD158a/h[1]	KIR2DL1 DS1	PE[1]	m-IgG1	EB6	BC	A09778	Direct
CD158b/j[1]	KIR2DL2/3 DS2	PE[1]	m-IgG1	GL183	BC	IM2278U	Direct
CD158e[1]	KIR3DL1	PE[1]	m-IgG1	DX9	BD	555967	Direct
CD158i[1]	KIR2DS4	PE[1]	m-IgG1	FES172	BC	IM3337	Direct
CD159a	NKG2A	PE-Cy7	m-IgG2b	z199	BC	B10246	Direct
CD159c	NKG2C	APC	m-IgG1	134591	R&D	FAB138A	Direct
CD183	CXCR3	AF647	m-IgG1	G025H7	Biolegend	353712	Direct
CD193	CCR3	PE	r-IgG2a	61828	R&D	FAB155P	Direct
CD197	CCR7	FITC	m-IgG2a	150503	R&D	FAB197F	Direct
CD198	CCR8	APC	r-IgG2b	191704	R&D	FAB1429A	Direct
n/a	CCR10	PE	r-IgG2a	314305	R&D	FAB3478P	Direct
n/a	CLA	APC	r-IgM	HECA-452	Miltenyi	130-098-573	Direct
n/a	CX3CR1	PE	r-IgG2b	2A9-1	Biolegend	341604	Direct
CD226	DNAM1	FITC	m-IgG1	DX11	BD	559788	Direct
CD314	NKG2D	APC	m-IgG1	1D11	BD	558071	Direct
CD335	NKp46	PE	m-IgG1	BAB281	BC	IM3711	Direct
CD336	NKp44	PE	m-IgG1	Z231	BC	IM3710	Direct
CD337	NKp30	PE	m-IgG1	Z25	BC	IM3709	Direct
n/a	NKp80	APC	m-IgG1	5D12	Biolegend	346708	Direct
n/a	ITGB7	APC	r-IgG2a	FIB504	BD	551082	Direct
n/a	Isotype m-IgG1	APC	m-IgG1	15H6	BC	731586	Direct
n/a	Isotype m-IgG1	FITC	m-IgG1	15H6	BC	731583	Direct
n/a	Isotype m-IgG1	PE	m-IgG1	X40	BD	345816	Direct
n/a	Isotype m-IgG2a	PE	m-IgG2a	X39	BD	349053	Direct
n/a	Isotype m-IgM	FITC	m-IgM	R4A3-22-12	BC	6602434	Direct
n/a	Isotype R-IgG2a	APC	r-IgG2a	eBR2a	eBioscience	17-4321-71	Direct
n/a	Isotype R-IgG2a	PE	r-IgG2a	54447	R&D	IC006P	Direct
n/a	Isotype R-IgM	APC	r-IgM	NIP/M-2	Southern	0120-11	Direct
n/a	Granzyme B	AF700	m-IgG1	GB11	BD	557971	Intracellular
n/a	Perforin	FITC	m-IgG2b	delta G9	Ancell	358-040	Intracellular
n/a	Tumor Necrosis Factor α	PE	m-IgG1	MAb11	BD	554513	Intracellular
n/a	Interferon-γ	FITC	m-IgG1	4S.B3	BD	554551	Intracellular

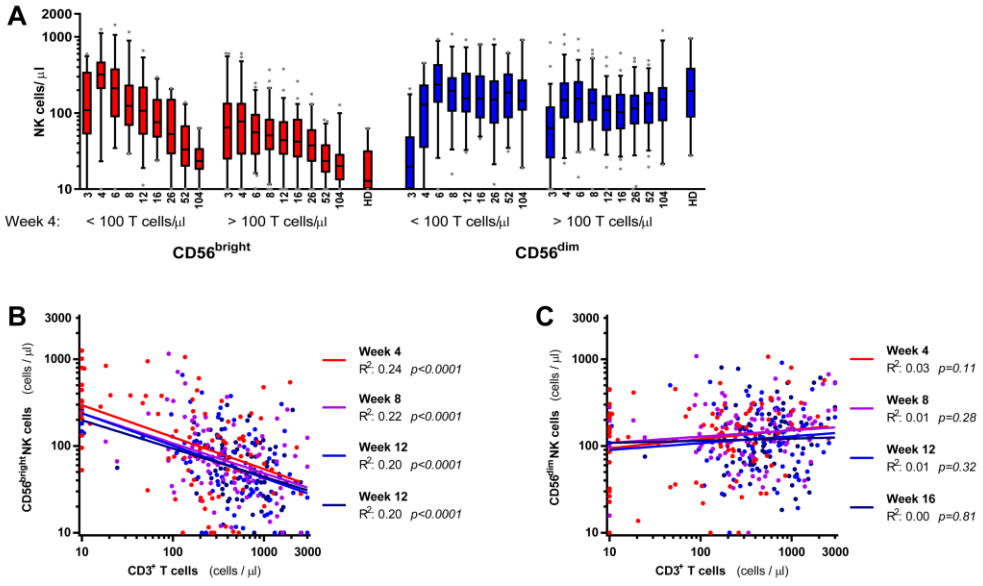

Figure 6.S1. Correlation between T cell and NK cell reconstitution after HSCT.

(A) Absolute cell numbers of CD56^{bright} (red) and CD56^{dim} (blue) NK cells at 3, 4, 6, 8, 12, 16, 26. 52 and 104 weeks after HSCT (n=93) and in healthy donors (n=16). Patients were devided in two groups based on T cell reconstitution < and > 100 cells/µl at 4 weeks after HSCT. Boxes: median and interquartile range, whiskers: 5-95 percentile, dots: outliers.

(B-C) Correlation of CD3+ T cell numbers with (A) CD56^{bright} NK cell numbers and (B) CD56^{dim} NK cell numbers at 4, 8, 12 and 16 weeks after hematopoietic stem cell transplantation (HSCT) in 93 patients. Statistics: Linear regression analysis on log-transformed data

Figure 6.S2 (next pages). Cell surface marker expression on CD56^{bright} and CD56^{dim} NK cells.
The expression of **(A)** chemokine receptors, **(B)** adhesion molecules and **(C)** NK cell receptors on CD56^{bright} (red) and CD56^{dim} (blue) NK cells at 3, 4, 6, 8, 12, 16, 26 and 52 weeks after HSCT (n=20) and healthy donors (HD, n=16). No expression of CCR1, CCR3, CCR4, CCR8, CCR9, CCR10, CXCR5 and CD103 was measured on NK cells (data not shown). Bars: mean +/- SEM, dots: individual patients. Expression: percentage of marker minus isotype control (%) or fluorescence intensity ratio of marker / isotype control (FI). Dotted line: normalized FI of isotype control. *p values:* Unpaired t test on log-transformed data. Comparison between healthy donor CD56^{bright} NK cells and post-transplant CD56^{bright} NK cells at week 4 (unless otherwise stated). *p values* are only shown when significant after Bonferroni-Holm correction for multiple comparisons. NS: not significant after Bonferroni-Holm correction.

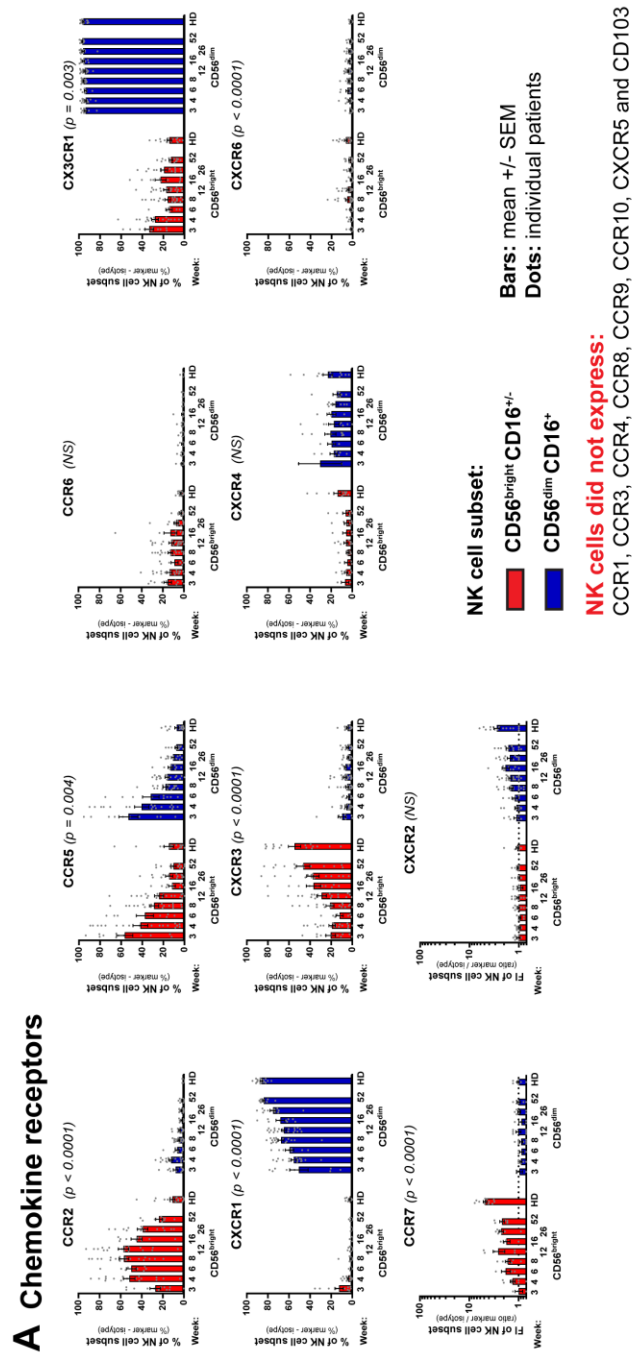

Figure 6.S2. Cell surface marker expression on CD56^{bright} and CD56^{dim} NK cells.

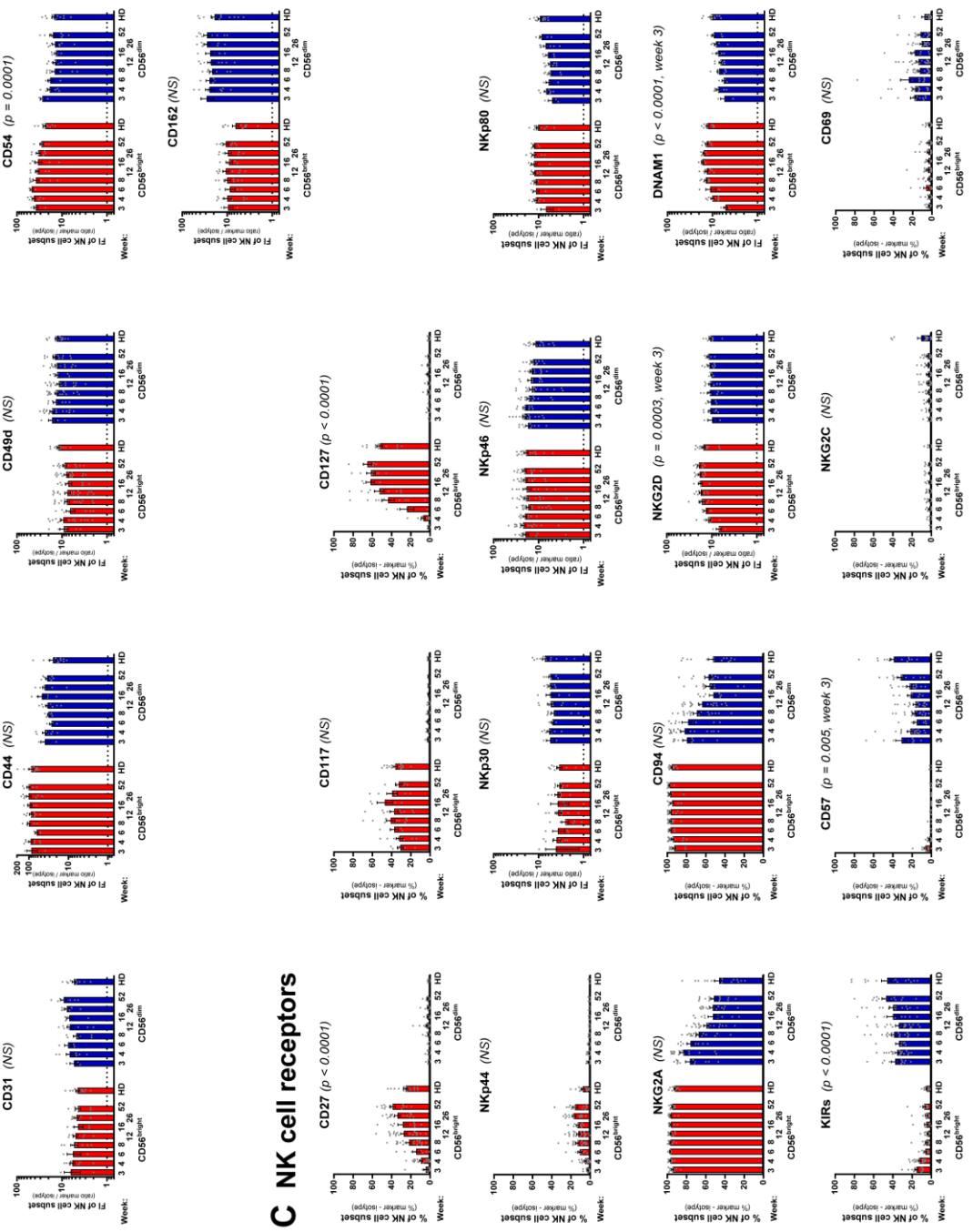

Figure 6.S2. Cell surface marker expression on CD56^{bright} and CD56^{dim} NK cells (continued).

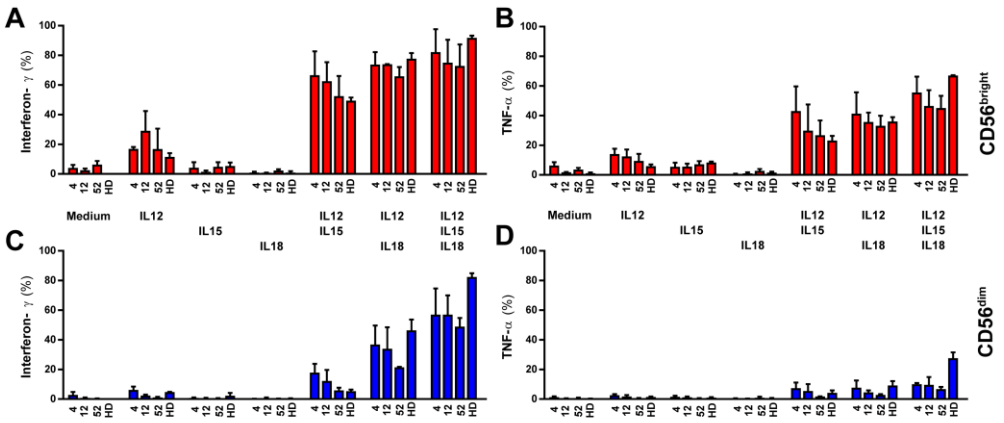

Figure 6.S3. Cytokine secretion of NK cells after HSCT.
Intracellular expression of interferon-γ **(A, C)** and TNF-α **(B, D)** in CD56^{bright} (red, A, B) and CD56^{dim} (blue, C, D) NK cells at 4, 12 and 52 weeks after HSCT (n=3) and healthy donors (n=2) cultured in absence or presence of (combinations of) IL12, IL15 or IL18. Bars: mean +/- SEM.

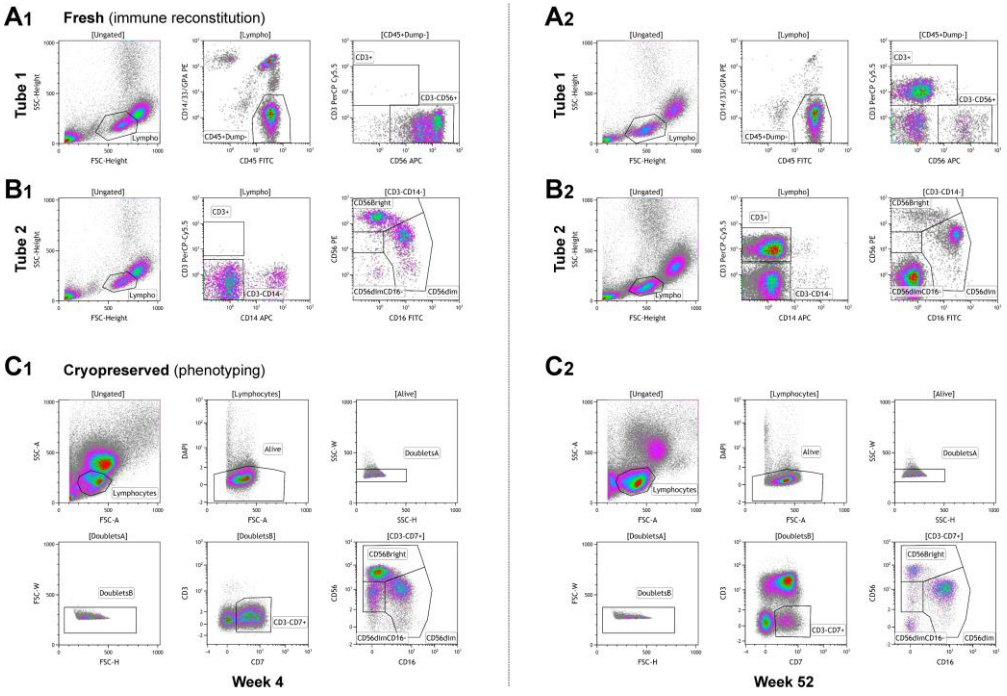

Figure 6.S4. Gating strategy.

The combination of flowcytometry on fresh PBMC, absolute leukocyte counts and full leukocyte differentiation was used to calculate absolute cell numbers of T cells, CD56^{bright} and CD56^{dim} NK cells. The expression of cell surface markers was evaluate on CD56^{bright} and CD56^{dim} NK cells using cryopreserved PBMC. An example of the gating strategy is shown for a (A-B) fresh and (C) cryopreserved sample at four weeks (A1-C1) and one year after HSCT (A2-C2).

(A) In tube 1, lymphocytes were defined as CD45+ CD33/CD235a/CD14- within the forward / sideward scatter lymphocyte gate. T-cells and NK cells were defined as CD3+ cells and CD3-CD56+ cells in the lymphocyte population, respectively.

(B) In tube 2, CD56^{bright}CD16$^{+/-}$ and CD56^{dim}CD16^{+} NK cells were gated within the CD3-CD14- lymphocyte gate.

(C) In cryopreserved samples, DAPI was used to exclude dead cells. CD56^{bright}CD16$^{+/-}$ and CD56^{dim}CD16^{+} NK cells were defined as living, non-doublet CD3-CD7+ lymphocytes expressing CD56 and/or CD16. CD56^{dim}CD16^{-} NK cells were excluded as they represented a separate population in cryopreserved but not in fresh PBMC.